New insights into large tropical tree mass and structure from direct harvest and terrestrial lidar

A. Burt[1], M. Boni Vicari[1], A. C. L. da Costa[2], I. Coughlin[3], P. Meir[3,4], L. Rowland[5] and M. Disney[1,6]

1. Department of Geography, University College London, UK
2. Instituto de Geosciências, Universidade Federal do Pará, Brazil
3. Research School of Biology, Australian National University, Australia
4. School of GeoSciences, University of Edinburgh, UK
5. College of Life and Environmental Sciences, University of Exeter, UK
6. NERC National Centre for Earth Observation (NCEO), UK

Abstract

A large portion of the terrestrial vegetation carbon stock is stored in the above-ground biomass (AGB) of tropical forests, but the exact amount remains uncertain, partly due to the difficulty of making direct, whole-tree measurements. We harvested four large tropical rainforest trees (stem diameter: 0.6–1.2 m, height: 30–46 m, AGB: 3960–18 584 kg) in a natural closed forest stand in East Amazonia, and measured above-ground green mass, moisture content and woody tissue density. We found approximately 40 % of green mass was water, and the majority of AGB was most often found in the crown, but varied from 42–62 %. Woody tissue density varied substantially intra-tree, with both height and radius, but variations were not systematic inter-tree. Terrestrial lidar data were collected pre-harvest, from which volume-derived AGB estimates were retrieved. These estimates were more accurate than traditional allometric counterparts (mean tree-scale relative error: 3 % vs. 15 %). Error in lidar-derived estimates remained constant across tree size, whilst error in allometric-derived estimates increased up to 4 −fold over the diameter range. Further, unlike allometric estimates, the error in lidar estimates decreased when up-scaling to the cumulative AGB of the four trees. Terrestrial lidar methods therefore can help reduce uncertainty in tree- and stand-scale AGB estimates, which would substantially advance our understanding of the role of tropical forests in the global carbon cycle.

1 Introduction

Forests in Amazonia are estimated to store in the region of 50–60 Pg of carbon in above-ground live vegetation [1–3], and are likely a small carbon sink, estimated at $0.25 \pm 0.3\,\mathrm{Pg\,C\,yr^{-1}}$, but appear to be trending toward becoming a carbon source [4]. The uncertainty in these values has implications for assessing the response of Amazonia to climate change and policy intervention.

Fundamental to remotely sensed estimates of Amazon-scale carbon stocks are the networks of calibration sites; censused forest stands where the above-ground biomass (i.e., the mass of above-ground live plant matter at 0 % moisture content, AGB) of each tree has been measured (the carbon content of biomass varies, but is often observed to be between 45–50 %) [5–7]. Arguably however, error in measurements of stand-scale AGB at these sites is often overlooked or underestimated, possibly because of the so-called 'fallacy of misplaced concreteness' [8].

To directly measure the AGB of a tree is difficult: it requires the tree to be harvested, and subsequent measurement of: i) green mass via weighing, and ii) the moisture content of the green mass. Consequently this is rarely done: there is not a single hectare of tropical forest on Earth for which AGB has been fully measured via direct measurement. Indeed, we could find just 10 large trees (stem diameter ≥ 0.6 m) in Amazonia whose AGB had been directly measured and recorded in the peer-reviewed English language literature, where data were disclosed [9]. This increased to 60 when direct weighing measurements of green mass were at least partially replaced with geometry-derived volume estimates [10–14].

In lieu of direct weighing, AGB must instead be estimated at these calibration sites using allometry [15]. Allometric models describe correlations between tree-scale AGB, and more readily measured tree variables (e.g., stem diameter). These models are themselves constructed from some underlying calibration (in-sample) data collected from destructively harvested trees, where AGB was measured concurrent with these variables. For tropical forests, models are usually constructed from population- or regional-scale data (i.e., pan-tropical or Amazonia) due to diversity [16, 17]. The most widely-used pan-tropical allometric models also include additional predictor variables beyond stem diameter, such as tree height and wood density, partly to reduce the standard error of these models (i.e., these predictor variables are correlated with AGB, whilst not perfectly correlated with diameter), and partly to enable capture of subtle systematic biogeographic variations in tree height [18] and wood density [19, 20].

Error in allometric-derived estimates of AGB is potentially large, and introduced during the selection, measurement and modelling of the calibration (in-sample) data, and the measurement of the out-of-sample data (i.e., the predictor variables of any tree outside the calibration data whose AGB is to be estimated). At the tree-scale, uncertainty in an allometric-derived estimate of AGB can be larger than the estimate itself [21], and furthermore, because variation in AGB increases with tree size due to the multiplicative nature of plant growth [22], uncertainty is a function of tree size. At the 1 ha stand-scale, random errors will begin to average out, but when each source is properly accounted for, uncertainty can remain upwards of 40 % [23]. Unknowable systematic errors likely increase these uncertainties further, regardless of scale, because of

amongst other reasons, inconsistent measurement error in the measurement of predictor variables between in- and out-of-sample data [24]. In absolute terms then, the uncertainty in the current best estimates of stand-scale AGB is potentially large, and relatively, a function of plot composition. These potential errors at calibration sites are concerning because they will propagate directly through to larger-scale estimates of AGB and carbon.

Recently, new alternative methods for estimating tree- and stand-scale AGB have been pioneered using terrestrial lidar data [25]. Modern terrestrial laser scanners enable capture of rich-but-unorganised point clouds that provide a millimetre-accurate 3D sample of observable elements in forested scenes [26]. Various tools and workflows have been developed to analyse these data: from the segmentation of point clouds representing individual trees [27], the classification of individual points as returns from either wood or leaf surfaces [28, 29], to the construction of quantitative structural models (QSMs) via shape fitting, which explicitly describe woody tree architecture [30, 31].

These methods enable retrieval of whole-tree green woody volume from lidar data that, combined with a value of density, enable estimation of tree-scale AGB (n.b., these estimates of volume are derived from sampling external woody surfaces, so they are unable to account for either internal cavities/rot, or the contribution of leaf material to volume). Throughout this paper we use the term 'whole-tree basic woody tissue density' to describe the required value of density, which is important to define. First, the lidar data provide a 3D sample of any particular tree in a green state (i.e., it is assumed cell walls are saturated, and lumina are filled with water), so to estimate dry mass (i.e., mass at 0 % moisture content) from green volume, a basic density (i.e., dry mass over green volume) is required. Second, this single value needs to account for the density of each woody tissue (i.e., periderm, phloem, xylem, cambium and pith) that fills the volume, weighted by the relative abundance of each tissue. Third, this value must also account for the intra-tree variations in the densities of these tissues, which have been observed to vary with both radius and height [32–35].

So the key questions surrounding these new lidar-derived estimates of AGB: Are these estimates more accurate than allometric counterparts? What is the error, both random and systematic, in these estimates? What are the sources of these errors? Whilst there are different approaches to answering these questions, including simulation experiments, the gold standard is comparing estimates, $\mathrm{AGB_{est}}$, with directly measured reference values, $\mathrm{AGB_{ref}}$.

To date, several studies have published such validation work. Calders et al. [36] collected both lidar and destructive measurements from 65 trees in *Eucalyptus* spp. open forest in Australia, and using their particular lidar data processing chain, found the coefficient of variation of the root mean square error in tree-scale $\mathrm{AGB_{est}}$ to approximate 16 %. Perhaps the most significant finding of this study was the absence of a correlation between error and scale (i.e., error in $\mathrm{AGB_{est}}$ was invariant of tree size). This is a potentially important differentiator between lidar- and allometric-based approaches, because it would suggest that when these lidar methods are up-scaled, stand-scale estimates would be independent of the stand and its composition.

For tropical forests, Momo Takoudjou et al. [37] acquired lidar and destructive data in Cameroon for 61 trees (mean stem diameter: 0.58 m, tree height: 34 m), and found the mean tree-scale relative error in AGB_{est} approximated 23 %. Gonzalez de Tanago et al. [38] also collected similar data in Guyana, Indonesia and Peru for 29 trees (mean stem diameter: 0.73 m), and found the coefficient of variation of the root mean square error in tree-scale AGB to approximate 28 %. In contrast to [36], error was observed to increase with tree size in both these studies. One possible explanation for this, and the overall increase in error, is the additional difficulty in acquiring lidar and destructive data in dense and remote tropical forests.

For example, in both [37] and [38], AGB_{ref} could not always be obtained from the direct measurement of green mass. Instead, for all trees [38], or for portions of large trees [37], mass was instead estimated from geometry: length and diameter measurements were converted into green volume estimates by assuming underlying tree structure could be represented by either a cylinder or conical frustum. Estimates of dry mass were then generated using an estimate of whole-tree basic woody tissue density obtained from either the harvested trees themselves [37], or from a global database [38]. That is, despite the significant advances both studies achieved, both were also limited in how accurately AGB_{ref} represented true above-ground biomass.

In this paper, we present the first comparison of lidar- and harvest-derived AGB for tropical trees, where the green mass of each tree was measured in its entirety. We decided to focus the experiment on collecting high quality and detailed measurements from a small sample of large trees, as opposed to collecting lower quality data from a larger sample. We harvested four large tropical rainforest trees in a natural closed forest stand in East Amazonia (stem diameter range: 0.6–1.2 m, tree height range: 30–46 m), and weighed their green mass. Also gathered were multiple discs from the stem and crown of each tree, on which woody tissue green-to-dry mass and volume ratios, and basic woody tissue density were measured. Terrestrial lidar measurements were collected from the four trees pre-harvest using a high-performance laser scanner after neighbouring trees and understory were cleared to minimise occlusion. Tree-scale AGB_{est} was retrieved from these data using a replicable and open-source processing chain. Crucially, these processing methods rely solely on the lidar data themselves for calibration (i.e., AGB_{est} was not *a priori* informed by AGB_{ref}).

In the results section, we initially present the reference data from the destructive harvest measurements. We also present some other interesting ecological insights from these data, including the moisture content of each tree, the distribution of AGB_{ref} between the stem and crown, and the intra-tree variations in basic woody tissue density. We then present the lidar data, and quantify the error in AGB_{est} retrieved from these data. We show how these errors compare with those obtained from allometric approaches. We then discuss the wider implications of these data for improving tropical forest AGB estimates and related ecological understanding.

2 Methods

Destructive and non-destructive data were collected from four large trees (designated T1-T4, pictured in figure 1) in Floresta Nacional de Caxiuanã, Pará, Brazil, during September and October 2018. These data are open-access and distributed under the terms of the Creative Commons Attribution 4.0 International Public License (CC BY 4.0). Persistent identifiers for these data are available in the data accessibility section.

2.1 Site metadata

The approximate coordinates of the site in the WGS-84 datum are $-1.798°$, $-51.435°$. The site is classified as moist, terra firme, pre-quaternary, lowland, mixed species, old-growth tropical forest. Mean annual rainfall is 2000–2500 mm, with a dry season between June and November. Soils at a nearby long-term through-fall exclusion experiment (approximately 7 km from the site) are yellow oxisol, composed of 75–83 % sand, 12–19 % clay and 6–10 % silt [39, 40].

2.2 Tree selection

We determined tree selection should principally ensure there was some range in the values of stem diameter and tree height. Other considerations influencing selection was a bias towards those that appeared healthy and with a complete crown, felling (in particular, that no large trees were occupying the felling area), and also permission from the land owners. The four selected trees matching these criteria were identified to species, and foliage/fruit samples retained to confirm taxonomic identity at the Museu Paraense Emílio Goeldi, Belem, Pará. Nearby vegetation surrounding each tree was removed, including complete clearing (of small bushes and saplings) of the felling area, to enable detailed non-destructive and destructive activities.

2.3 Non-destructive measurements

Stem diameter was measured using a circumference/diameter tape. Measurement was made at either 1.3 m above-ground (T4), or 0.5 m above-buttress (T1, T2 and T3). Lidar data were collected using a RIEGL VZ-400 terrestrial laser scanner. A minimum of 16 scans (upright and tilt) were acquired from 8 scan positions around each tree. The angular step between sequentially fired pulses was 0.04°, and the distance between scanner and tree varied. This arrangement provided a 45° sampling arc around each tree, and a complete sample of the scene from each position. The laser pulse has a wavelength of 1550 nm, a beam divergence of 0.35 mrad, and the diameter of the footprint at emission is 7 mm. The instrument was in 'High Speed Mode' (pulse repetition rate: 300 kHz), 'Near Range Activation' was off (minimum measurement range: 1.5 m), and waveforms were not stored.

2.4 Destructive measurements

The various field and laboratory measurements are described below. Included in the destructive dataset are photographs illustrating these measurements.

2.4.1 Field measurements

The location, height and green mass of the four trees were measured in the field, and multiple discs were also collected from each tree. Trees were cut at a height of approximately 1 m above-ground, and felled onto tarpaulin. A STIHL MS 650 chainsaw with a 20" bar length and 13/64" chain loop was used for cutting. Tree height (including stump) was measured with a surveyor's tape measure, and GPS data were acquired from the centre of the stump using a Garmin GPSMAP 64st.

Two Adam LHS 500 crane scales (capacity: 500.0 kg, division: 0.1 kg) were suspended from nearby trees to measure green mass. Calibration certificates are included in the destructive dataset certifying both instruments conformed (pre-delivery) to various tests of repeatability, linearity and hysteresis. Post-campaign, the consistency of measurements between instruments was tested using a variety of different masses, and also the laboratory balance with internal calibration weights described in the following subsection.

Green mass was assigned to either the stem or crown pool, where the stem was defined as the bole from flush with the ground up to the first fork. The stem was cut into manageable sections; the length and diameter of each section was measured using a circumference/diameter tape (lengths varied from 0.15–0.54 m for T2 and T4 respectively), and then weighed. Remaining stump material was cut flush with the ground and weighed. Large branches were measured similar to the stem, and fine branching and leaf material were collected in large sacks and weighed. These green mass measurements commenced immediately post-felling, but two, four, four and two days were required to complete measurement of T1-T4 respectively.

Discs of approximately 50 mm thickness were collected from the stem and crown of each tree. Four discs were collected from the stem: at 1.3 m above-ground, and at 25 %, 50 % and 75 % the length of the stem. Up to three discs were also collected from the mid-points of 1st, 2nd and 3rd order branches. A minimum of 11 discs was collected per tree. Figure 2 shows the discs collected from T4.

2.4.2 Laboratory measurements

Discs were reduced to subsamples using a consistent approach: for any particular disc, they were cut as guided by parallel chords straddling above and below the major axis, each with approximate dimensions of 150 mm x 50 mm x 50 mm. That is, each set of subsamples covered the diameter of their respective disc (i.e., each set included periderm, phloem, cambium, xylem and pith tissues). Figure 2 shows the sets of subsamples cut from the discs of T4.

The mass and volume of each subsample was measured whilst in both a green and dry state. Mass measurements were made using an Adam NBL4602i Nimbus Precision balance (capacity: 4600 g, division: 0.01 g). This balance contains internal calibration weights, and a calibration certificate is available in the harvest dataset certifying this instrument conformed (pre-delivery) to external tests of repeatability, eccentric loading, linearity and hysteresis. Volume measurements were made using the balance via Archimedes' principle. Subsamples were considered in a green

state after soaking for 48 hours. They were considered in a dry state once a constant mass had been attained whilst drying in an oven at 105 °C.

In the original campaign, the green volume of subsamples was not measured (necessary for calculating basic woody tissue density). We returned to the harvest site in October 2019 and collected new discs and subsamples from the wood piles of each tree using the methods described above. The integrity of the wood was verified by comparing measurements of woody tissue green-to-dry mass ratio and dry woody tissue density. The green volume of the original subsamples was retrospectively calculated using the mean woody tissue green-to-dry volume ratio from these new subsamples.

2.5 Woody tissue green-to-dry ratios and density

Whole-tree woody tissue green-to-dry mass and volume ratios were estimated for each tree from measurements on the subsamples using a mass-weighted approach. These two parameters were calculated by weighting the mean from subsamples in each pool (stem and crown), with the green mass in each pool. Whole-tree basic woody tissue density was estimated using three approaches: i) Mass-weighted. ii) Stem, which was calculated from the mean of the two outer subsamples from the stem disc at 1.3 m above-ground. This second approach was intended to mimic values acquired via boring (i.e., measurements on cores). iii) Literature, where values were acquired from the Global Wood Density Database [41], whereby the value considered was the mean of matched species-level entries.

2.6 Above-ground biomass

2.6.1 Reference values

Reference above-ground biomass, AGB_{ref}, was calculated from whole-tree green mass and the mass-weighted estimate of whole-tree woody tissue green-to-dry mass ratio. Mass lost in swarf from chainsaw cuts was partially accounted for using a volume-derived approach (stem only). A green cut volume was estimated for each of the manageable stem sections by assuming it could be represented by a cylinder. An average cut width of 8.4 mm (approximately 60 % thicker than the chain loop) was estimated from multiple caliper measurements. Lost dry mass was estimated from these green volumes using the mass-weighted estimate of green woody tissue density and the estimate of woody tissue green-to-dry mass ratio. These corrections increased AGB_{ref} by 0.7 %, 1.8 %, 0.7 % and 0.7 % for T1-T4 respectively.

2.6.2 Lidar estimates

Estimated above-ground biomass, AGB_{est}, was retrieved from the lidar data using the software described below. With the exception of the initial step, these tools are open-source, and persistent identifiers are available in the software accessibility section. Individual lidar scans were registered onto a common coordinate system using *RiSCAN PRO* (v2.7.0) [42]. The point clouds of the individual trees were extracted from the larger-area point clouds using *treeseg* (v0.2.0) [27].

Returns from leaf material were segmented from these tree-level point clouds after returns from wood and leaf surfaces were classified using *TLSeparation* (v1.2.1.5) [28]. Points from buttresses were then manually removed using *CloudCompare* (v.2.10.3) [43]. Quantitative structural models (QSMs) were constructed from the tree-level point clouds using *TreeQSM* (v2.3.2) [30]. Input parameters to *TreeQSM* were automatically selected using *optqsm* (v0.1.0). $\mathrm{AGB_{est}}$ was calculated from QSM-derived whole-tree green woody volume and the mass-weighted estimate of whole-tree basic woody tissue density.

2.6.3 Allometric estimates

$\mathrm{AGB_{est}}$ was calculated using the 2 −parameter model described in Chave et al. [16] (equation 4, three predictor variables: stem diameter, D (cm), tree height, H (m), and basic wood density, ρ ($\mathrm{g\,cm^{-3}}$)). This model is constructed from measurements collected on 4004 destructively harvested trees from across the tropics, and takes the form:

$$\mathrm{AGB_{est}} \;=\; 0.067(D^2 H \rho)^{0.976} \tag{1}$$

Appendix A in the Supplementary Material considers our decision to select this particular model to represent the allometric approach.

2.6.4 The performance of estimates

To describe the performance of lidar- and allometric-derived $\mathrm{AGB_{est}}$, we use the terms random error, systematic error, total error, precision, trueness, accuracy, bias and uncertainty. For the avoidance of doubt, these terms are used strictly within the ISO 5725 and BIPM definitions [44]. Error, ε, in $\mathrm{AGB_{est}}$ is defined as:

$$\varepsilon = \mathrm{AGB_{est}} - \mathrm{AGB_{ref}} \tag{2}$$

Relative error is defined as:

$$RE = \frac{|\varepsilon|}{\mathrm{AGB_{ref}}} \tag{3}$$

Mean tree-scale relative error is defined as:

$$MRE = \frac{1}{n}\sum_{i=1}^{n} RE_i \tag{4}$$

Mean error is used to quantitatively express trueness:

$$ME = \frac{1}{n}\sum_{i=1}^{n} \varepsilon_i \tag{5}$$

The standard deviation of the error is used to quantitatively express precision:

$$STDEV = \sqrt{\frac{1}{n}\sum_{i=1}^{n}(\varepsilon_i - \bar{\varepsilon})^2} \tag{6}$$

Root mean square error is used to quantitatively express accuracy:

$$RMSE = \sqrt{\frac{1}{n}\sum_{i=1}^{n}\varepsilon_i^2} \tag{7}$$

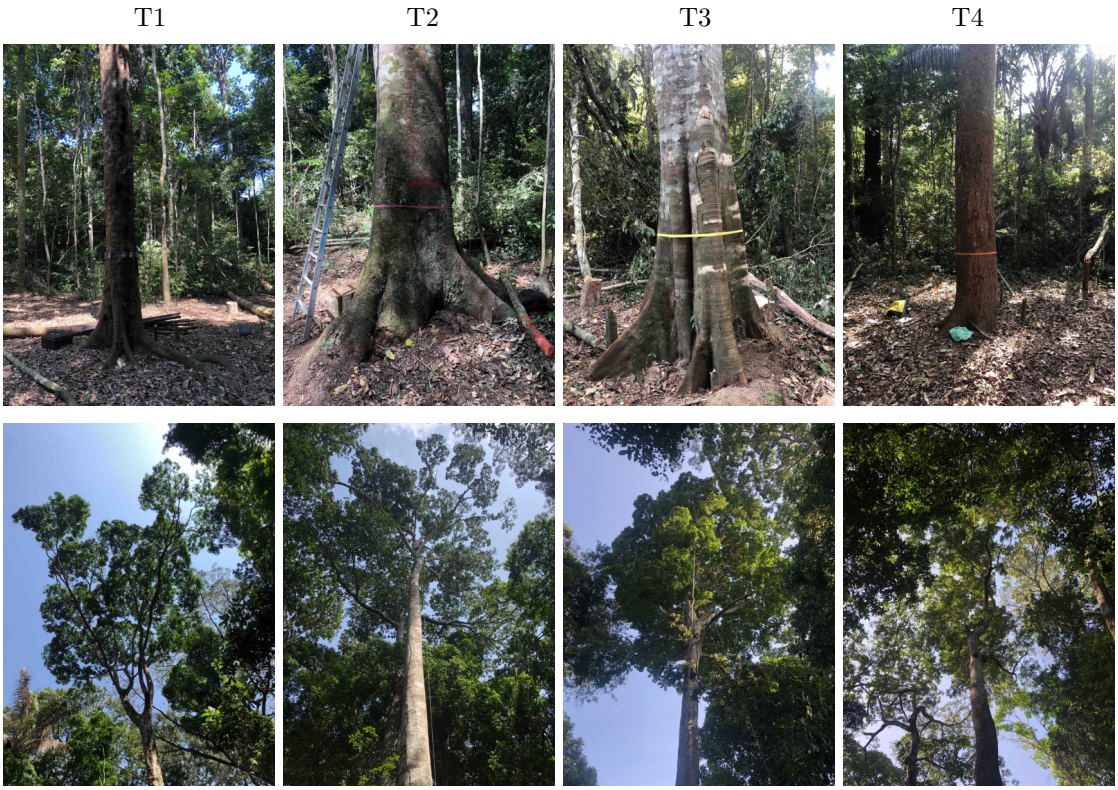

Figure 1: Stem and crown photographs of each harvested tree. Left to right: T1 (*Inga alba* (Sw.) Willd.), T2 (*Hymenaea courbaril* L.), T3 (*Tachigali paniculata* var *alba* (Ducke) Dwyer) and T4 (*Trattinnickia burserifolia* Mart.).

Figure 2: The discs collected from T4 (upper left). Four were taken from the stem at 1.3 m above-ground, and at 25 %, 50 % and 75 % the length of the stem. Eight were taken from the mid-points of 1st, 2nd and 3rd order branches. Each disc was then reduced to a set of subsamples: for any particular disc they were cut as guided by parallel chords above and below the major axis (lower). It is noted that each set of subsamples included periderm, phloem, cambium, xylem and pith tissues. The upper right photograph shows all T4 subsamples.

3 Results

3.1 Destructive measurements

Above-ground green mass of the four trees ranged from 6808–29 511 kg, totalling 59 005 kg (table 1). The disc-derived estimates of whole-tree woody tissue green-to-dry mass ratio ranged from 1.62–1.73 , implying approximately 40 % of green mass was water. Whole-tree woody tissue green-to-dry volume ratio ranged from 1.11–1.14 , indicating green woody tissue volume shrank, on average, by 12 % after drying. AGB_{ref} ranged from 3960–18 584 kg, totalling 36 458 kg. The proportion of AGB_{ref} distributed between the stem and crown varied between trees, with the crown mass ratio ranging from 0.42–0.62 , but for three out of four, the majority was found in the crown (figure 3).

The mass-weighted estimates of whole-tree basic woody tissue density returned values for the four trees that ranged between 568–769 $kg\,m^{-3}$. The values generated from the other direct approach using disc measurements (stem), and intended to mimic values acquired via boring, were consistent with mass-weighted counterparts, with a maximum percentage difference of 3 % (table 1 and figure 4). Non-direct literature-derived values were less consistent: for T1 and T2 they were reasonably close, but were substantially lower than mass-weighted estimates in both T3 and T4, with a percentage difference of 3 %, 3 %, 14 % and 21 % for T1-T4 respectively.

Within tree, woody tissue density varied substantially (figure 4): the maximum observed difference in the basic woody tissue density of subsamples collected throughout each tree was 40 $kg\,m^{-3}$, 79 $kg\,m^{-3}$, 166 $kg\,m^{-3}$ and 156 $kg\,m^{-3}$ for T1-T4 respectively. Overall, basic woody tissue density decreased with height in T2, increased in T3 and T4, and remained largely invariant in T1. A pronounced decrease in basic woody tissue density was observed towards the centre of each disc in T3, which was not seen in the other trees.

3.2 Non-destructive measurements

The downsampled lidar data comprised a minimum 2.6 million points per tree (figure 3). The QSMs constructed from the woody point clouds are shown in figure 5. Combining QSM-derived whole-tree green woody volume with the mass-weighted estimate of whole-tree basic woody tissue density provided AGB_{est} with a mean tree-scale relative error of 3 % (table 2). Relative error in up-scaled AGB_{est} (i.e., the error in the cumulative AGB_{est} of the four trees) was 1 %. For the pan-tropical allometric estimates, mean tree-scale relative error was 15 %, and relative error in up-scaled AGB_{est} was 15 %.

Overall, the lidar methods returned more accurate predictions than allometry (table 2). Precision-wise (random error), the standard deviation of the error in lidar-derived estimates was considerably smaller: 185 kg vs. 2523 kg. The lidar-derived estimates were also more true (systematic error), but did tend to be underestimates (mean error: −70 kg).

The approach to estimating whole-tree basic woody tissue density was an important determinant of error (figure 6). For the lidar methods, the values derived from direct disc measurements provided predictions with the smallest error: mean tree-scale relative error in AGB_{est} using

mass-weighted, stem and literature estimates of whole-tree basic woody tissue density was 3 %, 4 % and 9 % respectively. This was more variable for allometric-derived predictions, with mean tree-scale relative error remaining largely constant across the three approaches.

ID	Species	Coords (°)	D (m)	H (m)	Green mass (kg)	Dry mass (AGB_{ref}) (kg)	Whole-tree woody tissue green-to-dry ratio		Whole-tree basic woody tissue density ($kg\,m^{-3}$)		
							Mass	Volume	Mass-weighted	Stem	Literature
T1	*Inga alba* (Sw.) Willd.	-1.79851 -51.43463	0.647	29.8	6808.2	3960.1	1.731	1.169	567.6	574.6	586.1
T2	*Hymenaea courbaril* L.	-1.79832 -51.43479	1.179	46.2	29 511.0	18 584.2	1.617	1.126	768.9	786.7	792.4
T3	*Tachigali paniculata* var. *alba* (Ducke) Dwyer	-1.79914 -51.43451	0.905	34.9	13 697.5	8392.6	1.643	1.137	639.0	655.1	554.5
T4	*Trattinnickia burserifolia* Mart.	-1.79550 -51.43433	0.697	35.2	8988.6	5521.1	1.640	1.113	567.0	561.9	460.0

Table 1: Parameters of the four harvested trees. A complete description of the measurements is available in the methods section.

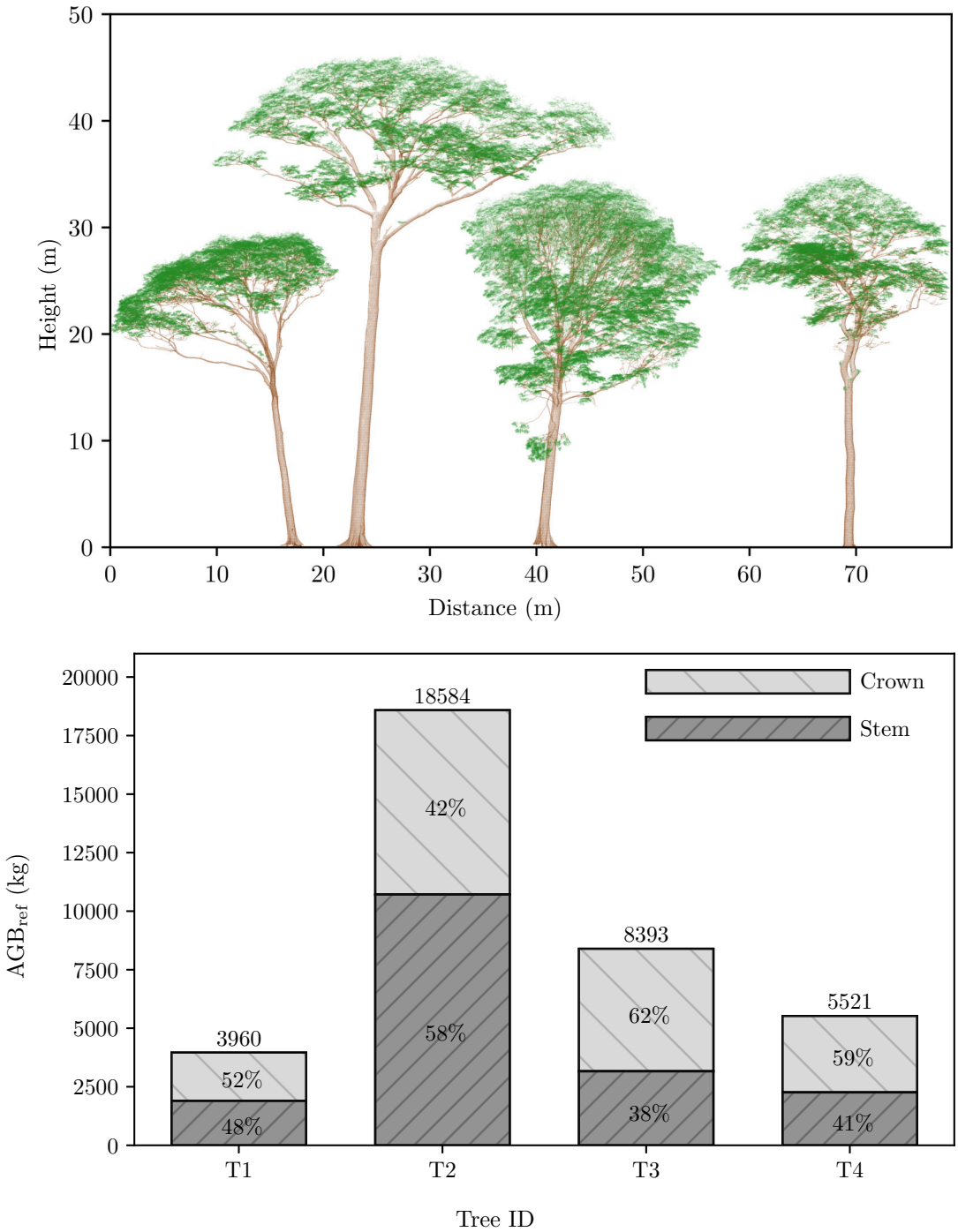

Figure 3: The terrestrial lidar point clouds of the four harvested trees (upper subfigure, shown to scale, left to right: T1-T4). Points were classified as returns from wood (brown) and leaf (green) surfaces using *TLSSeparation*. Reference above-ground biomass, AGB_{ref}, derived from direct weighing measurements, totalled 36 458 kg across the trees. The lower subfigure presents the distribution of AGB_{ref} between the stem and crown of each tree.

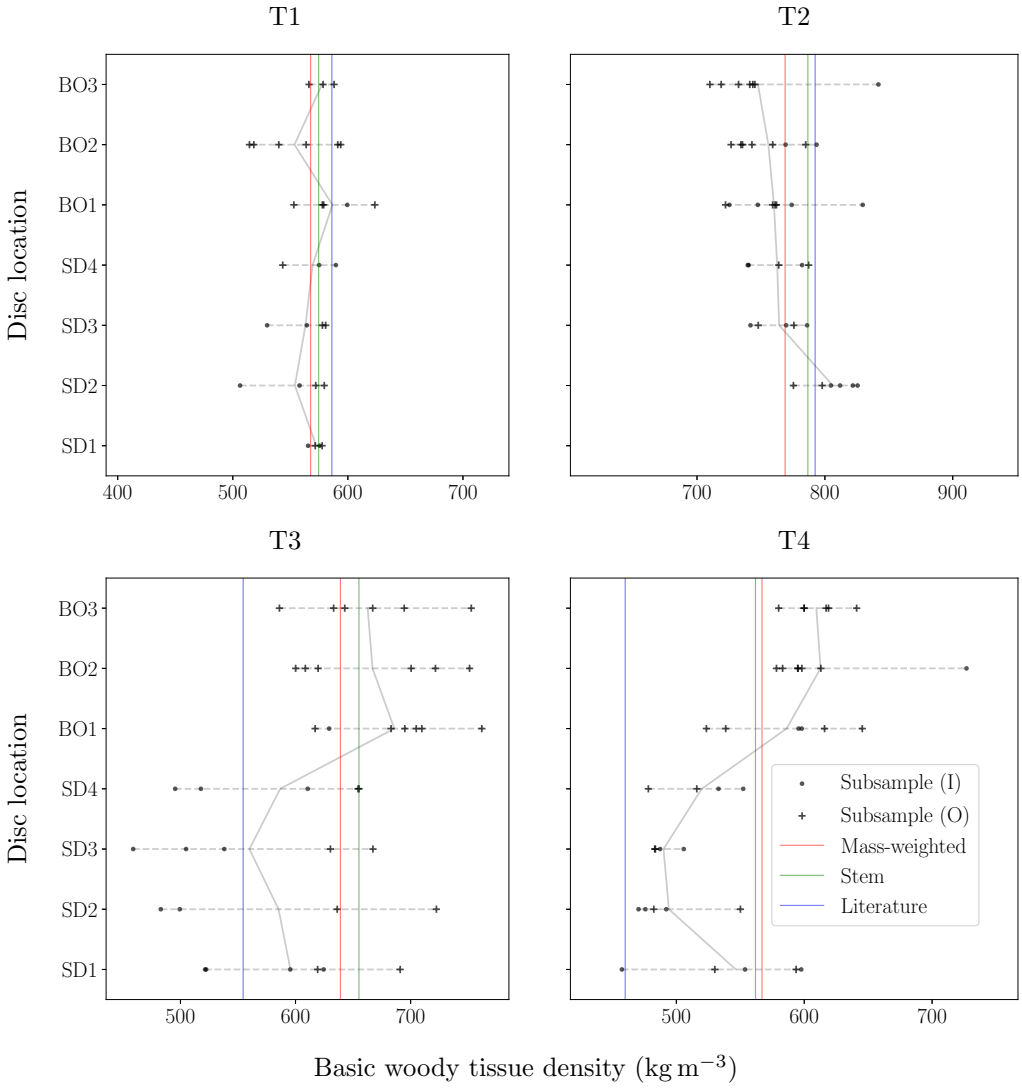

Figure 4: Intra-tree variations in basic woody tissue density with height. Discs were collected from the stem of each harvested tree at 1.3 m above-ground, and at 25 %, 50 % and 75 % along the length of the stem (SD1-SD4). Discs were also taken from the midpoints of 1st, 2nd and 3rd order branches (BO1-BO3). A minimum of 11 discs was collected per tree. Discs were subsequently reduced to subsamples using a consistent approach (figure 2), and any given set of subsamples covered the full extent of each disc. Each data point represent a measurement of basic woody tissue density on a subsample: crosses represent outer subsamples (i.e., they included periderm, phloem and cambium tissues), and dots represent inner subsamples. Also shown is the range of the values per section (dotted grey line), and the linear interpolation between sections (solid grey line). The vertical lines represent the estimates of whole-tree basic woody tissue density derived from the considered approaches: mass-weighted (red), stem (green) and literature (blue).

Figure 5: Quantitative structural models of the four harvested trees (left to right: T1-T4), which were automatically constructed from the woody point clouds shown in figure 3 using *TreeQSM* and *optqsm*.

ID	AGB_{ref} (kg)	Terrestrial lidar			Pan-tropical allometry		
		AGB_{est} (kg)	Error (kg)	Relative error (%)	AGB_{est} (kg)	Error (kg)	Relative error (%)
T1	3960.1	3673.8	−286.3	7.2	3644.9	−315.2	8.0
T2	18 584.2	18 414.5	−169.7	0.9	24 261.0	5676.8	30.5
T3	8392.6	8604.6	212.0	2.5	9190.9	798.3	9.5
T4	5521.1	5485.1	−36.0	0.7	4953.7	−567.4	10.3
Mean	-	-	-	2.8	-	-	14.6
Summed	36 458.0	36 177.9	−280.1	0.8	42 050.5	5592.5	15.3

Error type	Performance characteristic	Quantitative metric	Estimation method	
			Terrestrial lidar	Pan-tropical allometry
Systematic	Trueness	Mean error (kg)	−70.0	1398.1
Random	Precision	Standard deviation of the error (kg)	185.3	2523.2
Total	Accuracy	Root mean square error (kg)	191.1	2884.7

Table 2: Comparing the performance of lidar- and allometric-derived estimates of above-ground biomass, AGB_{est}, with harvest-derived reference above-ground biomass, AGB_{ref}. Estimates from both approaches were calculated using the mass-weighted estimate of whole-tree basic woody tissue density. The upper table reports the error in these estimates. Mean relative error is the average of tree-scale relative errors. Summed values refer to the cumulative AGB of the four trees. The lower table quantifies the performance of these estimates.

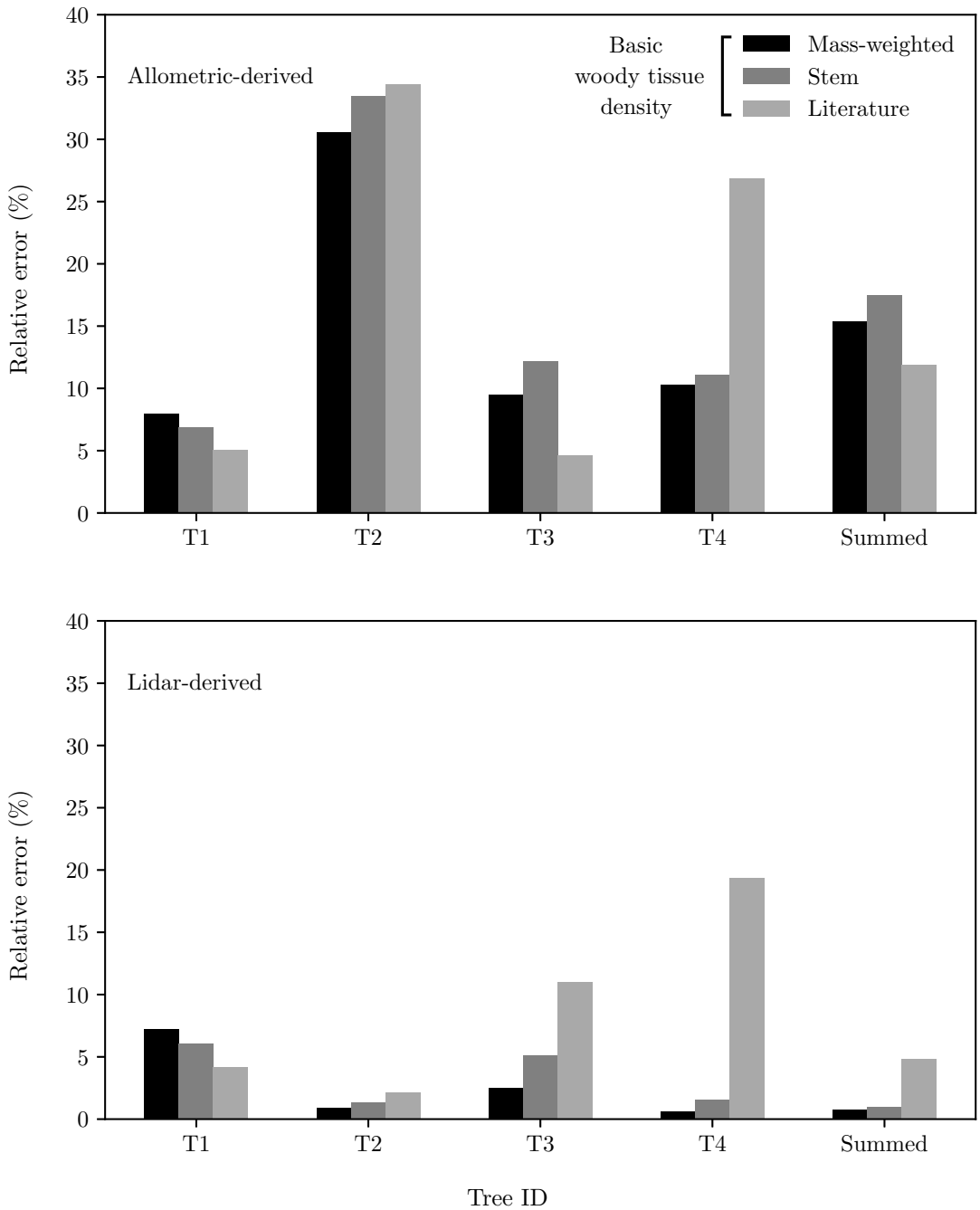

Figure 6: The impact of different approaches to estimating whole-tree basic woody tissue density on relative error in allometric- (upper) and lidar-derived (lower) estimates of above-ground biomass. The mass-weighted, stem and literature values reported in table 1 were used to calculate AGB_{est}.

4 Discussion

Direct measurements on the four harvested trees found AGB_{ref} to total 36 458 kg. Estimates from the lidar- and allometric-based methods totalled 36 178 kg and 42 051 kg respectively. The mean tree-scale relative error in these estimates was 3 % and 15 % respectively. Aside from an overall lower error term, lidar-derived estimates provided two further advantages. i) Error in AGB_{est} did not increase with tree size, and ii) error in AGB_{est} reduced when up-scaling from the tree-scale, to the cumulative of the four trees.

The destructive and non-destructive measurements also provided an important insight into the considerable variability in large tropical tree structure. We found the distribution of AGB between the stem and crown of each tree varied widely, with the crown mass ratio ranging from 0.42–0.62 . There was also variation in the mass-weighted estimates of whole-tree basic woody tissue density, which ranged from 567–769 $kg\,m^{-3}$. But more interesting perhaps were the intra-tree variations in woody tissue density, both with height and within disc, and that these variations were not systematic between trees. Less variable were the mass-weighted estimates of whole-tree woody tissue green-to-dry mass and volume ratios: we found green mass moisture content varied from 39–42 %, and green woody tissues shrank by 10–14 % after drying.

4.1 Terrestrial lidar methods reduce uncertainty in above-ground biomass

In the introduction we noted that errors in pan-tropical allometric-derived tree-scale AGB_{est} are often positively correlated with tree size, and that uncertainty from random error can remain upwards of 40 % at the 1 ha stand-scale [23, 24]. Uncertainty then, in the current best estimates of stand-scale AGB, is potentially large absolutely, and relatively, a function of plot composition. These uncertainties form the current minimum uncertainty in larger-scale estimates of AGB (e.g., Amazonia), because such estimates are themselves invariably reliant upon calibration from forest stands characterised by allometry. The results presented here suggest terrestrial lidar methods have the potential to reduce uncertainty in tree- and stand-scale AGB estimates by more than an order of magnitude, which would help to produce significantly more accurate estimates of larger-scale carbon stocks.

Overall, lidar-derived AGB_{est} provided a 15-fold increase in accuracy over allometric counterparts (RMSE difference, lower table 2). There were two important characteristics that further differentiated lidar and allometric approaches. i) Error in lidar-derived AGB_{est} was not positively correlated with tree size: relative error in the smallest and largest tree was 7 % and 1 % respectively (vs. 8 % and 31 % for allometric-derived estimates). ii) Error in lidar-derived AGB_{est} reduced when up-scaling from the tree-scale to the cumulative of the four trees: mean tree-scale relative error was 3 %, and the relative error in cumulative AGB_{est} was 1 % (vs. 15 % and 15 % for allometric-derived estimates). This second point is important because it potentially suggests errors themselves are not strongly correlated with one another (i.e., error in these estimates is predominately random). If these characteristics from our small sample of four trees were to persist when up-scaling to the stand-scale, then the error in lidar-derived estimates of stand-scale

AGB would be independent of the size of the trees comprising the stand, and would reduce as the number of trees within the stand increases.

The lidar-based estimates presented here were also substantially more accurate than those from previously published validation studies, where lidar-derived estimates were accompanied by harvest data. As described in the introduction, the two studies specific to tropical forests are those of Momo Takoudjou et al. [37] and Gonzalez de Tanago et al. [38]. The mean tree-scale relative error in lidar-derived AGB_{est} exceeded 20 % in both these studies (vs 3 % observed here). Because lidar-derived estimates are generated from explicit 3D models of tree architecture, errors arise from two sources: the estimation of volume, and the estimation of density. As discussed below, recent advances in processing methods have significantly reduced error in estimating whole-tree green woody volume. However, knowledge gaps remain, particularly in the estimation of whole-tree basic woody tissue density. These knowledge gaps will require filling before lidar-derived estimates are considered both consistently true and precise.

4.1.1 Estimating whole-tree green woody volume from point clouds

Time-of-flight laser scanners estimate the range to targets illuminated by the laser pulse, from timing measurements of returned radiation. A complex chain of methods are required to go from range estimates, to volumes. Sources of error in these methods can be broadly classified into two categories: those related to data acquisition, and those related to data processing.

Occlusion is an important source of error in the first category (i.e., tree components that are obscured by foreground objects). The impacts of occlusion on data quality are driven by multiple factors including the physical complexity of the scene, instrument parameters (e.g., beam divergence), increasing distance between sequentially fired pulses with range, and the user-defined sampling pattern (e.g., the location and number of scans within the scene, and the angular resolution). Another source of error in this category is the inability to collect information from inside the tree: that is, the impact on volume from internal rot/cavities is not accounted for. Other sources of error include the instrument itself (including sensitivity and ranging accuracy), as well as environmental impacts including wind and rain.

Sources of error in the second category are specific to the particular processing chain, but here would include those arising from: i) the registration of individual scans onto a common coordinate system, ii) the segmentation of individual trees from the larger-area point cloud, iii) the classification of points as returns from wood or leaf surfaces, iv) the manual removal of points from buttresses, and v) the approach to constructing quantitative structural models (e.g., cylinders were used to model structure).

It is not possible here to attribute the observed differences in AGB_{est} and AGB_{ref} to any of these sources. Indeed, attributing error to either top-level error source (i.e., the estimate of volume or density) is difficult. That is, we cannot explicitly explain the error because we do not have control over these individual sources, and because these errors are often correlated in complex ways (e.g., occlusion will affect the goodness of a cylinder fit).

However, we have demonstrated that given high-quality (occlusion minimised) terrestrial lidar data, the currently available open-source processing tools are capable of automatically generating estimates of large tropical whole-tree AGB to within a few percent of reference measurements, despite these potential sources of error in volume estimation. We think the recent development of wood-leaf separation algorithms has been a particularly important step forward in enabling this [28, 29]. Appendix B in the Supplementary Material helps to demonstrate this, where we show the inclusion of points returned from leafy surfaces will significantly interfere with the methods used here for woody reconstruction. We show that the segmentation of leafy returns from the tree-level point clouds reduced relative error in cumulative AGB_{est} from 41 %, to 6 %. We recommend then, that wood-leaf separation algorithms are a necessary and critical component for accurately retrieving AGB_{est} from high-quality and occlusion minimised terrestrial lidar data collected in evergreen forests, or so-called 'leaf-on' point clouds.

4.1.2 The more tricky issue of density

The other top-level source of error in lidar-derived AGB_{est} is in the estimation of whole-tree basic woody tissue density. As described in the introduction, if we were to assume a lidar estimate of a tree's green woody volume is error free, then to convert this into an unbiased estimate of AGB (assuming the contribution by leaf material to AGB is negligible), the whole-tree basic woody tissue density is required. We have intentionally used this very specific, albeit rather cumbersome term throughout the paper, because it is required to: i) convert a green volume into a dry mass, ii) account for the density of each woody tissue filling the volume, by the relative abundance of each tissue, and iii) account for the variations in woody tissue density throughout the tree.

However, direct measurement of whole-tree basic woody tissue density is impracticable for most trees because it can only be achieved via whole-tree weighing and water displacement. In this experiment, the measurement that closest resembled this value (and is similarly impracticable without destructive harvest) was the mass-weighted estimate of whole-tree basic woody tissue density (i.e., weighting the mean basic woody tissue density from the disc subsamples in each pool, by the green mass in each pool). This particular measurement helped to illustrate how the various practicable approaches to obtaining an estimate of whole-tree basic woody tissue density introduced error into lidar-derived AGB_{est} (figure 6).

For example, the approach intended to mimic measurements on cores acquired from boring (i.e., the approach termed stem, which was calculated from the mean basic woody tissue density of the two outer subsamples (approximate depths of 150 mm) collected from the stem disc at 1.3 m above-ground), increased mean tree-scale relative error from 3 %, to 4 %. Similarly, when we used values from the Global Wood Density Database [41], error increased to 9 %. We note however that a recent study highlighted values in this database might overstate some entries by approximately 3 %, which could partly explain some of these differences [45].

The key point then, is that whenever non-destructive AGB estimates are required, the only ways to currently obtain an estimate of whole-tree basic woody tissue density are through pub-

lished values or coring. The question is, are there any reliable methods to account for error in lidar-derived AGB_{est} that arises from the inability to directly measure whole-tree basic woody tissue density?

One approach is to convert values obtained from these methods into an estimate of whole-tree basic woody tissue density via some correction factor. Sagang et al. [33] and Momo Takoudjou et al. [35] have recently explored this approach for forests in Central Africa. In these studies, data from destructive measurements (n =130 and 822 trees respectively) were used to construct models to convert literature- or stem-derived values to more closely mirror whole-tree basic woody tissue density. [35] also captured lidar data for a subset of these harvested trees (n =58), and demonstrated systematic error in in-sample lidar-derived AGB_{est} reduced when these corrective models were applied.

It would be unreasonable to apply the published corrective models to the data collected here, given the substantial variation observed in woody tissue density within and between tropical regions [20]. It is however perhaps worth noting the top-level consequence had they been applied: our stem- and literature-derived estimates of whole-tree basic woody tissue density would have been pushed downward by approximately 21 % and 36 % respectively. This behaviour would have resulted in a substantial increase in the error of lidar-derived tree-scale AGB_{est} for all four trees (figure 4).

This is not to suggest such models are necessarily inappropriate at a larger-scale, (e.g., an equivalent model constructed from Amazonia data could be directionally correct), but at the out-of-sample tree- or stand-scale, it is impossible to determine whether they have a beneficial or detrimental impact on error in AGB_{est}. Another important consideration for these models in the context of Amazonia is the hyperdominance of certain species [46]. That is, it is not necessarily sufficient for these models to accurately correct a stem- or literature-derived value for the majority of species in the Amazon, if a large portion of Amazon-scale AGB is stored in a relatively small number of key species.

We would suggest then, there is currently no simple approach to account for error in lidar-derived AGB arising from the inability to measure whole-tree basic woody tissue density. In the longer-term, hopefully new non-destructive estimation methods will be pioneered, with interesting research ongoing using x-ray computed tomography [47] and genome sequencing [48, 49]. But in the meantime, our recommendation from the analysis of the data collected here, is that when viable, estimates acquired from direct measurements on the stems of trees are likely superior to those taken from the literature (mean tree-scale relative error in AGB_{est} of 4 % and 9 % respectively).

4.1.3 Improving uncertainty quantification

It is important to be able to assign meaningful uncertainty intervals to any estimate of AGB, whether allometric- or lidar-derived, and whether at tree- or stand-scale. That is, when such methods are applied to a tree or stand where destructive validation measurements are unavailable,

what is the uncertainty in subsequent estimates?

Our analysis of the data collected from a sample of four large tropical trees identified: i) error in lidar-derived AGB_{est} did not increase with tree size, and ii) error in AGB_{est} reduced when up-scaling from tree-scale, to the cumulative across the four trees. One plausible hypothesis: the error in terrestrial lidar-derived tree-scale AGB_{est} is independent of tree architecture, and predominately random. If this were provisionally confirmed, then to assign meaningful uncertainty intervals to out-of-sample tree- and stand-scale AGB_{est} would only require knowledge of the variance of the error.

To test this hypothesis, further destructive validation data similar to those collected here are required. In particular, it would be necessary to have some confidence that these new data attempted to capture the bounds of variability in tree architecture, and whole-tree woody tissue density. That is, these data would ideally be collected from a range of different forest types, species, size classes and crown forms.

If such data were to be collected, then priority should also be placed on two further considerations. First, on understanding how lidar data quality influence error. That is, how the instrument, sampling pattern and scene complexity increase random error variance and/or introduce systematic error. We note that the lidar data in this experiment were collected after neighbouring vegetation surrounding each tree was removed, meaning the quality of data is likely higher than equivalent data collected in a non-destructive setting.

Second, ideally the reference measurements should be collected from direct measurement of green mass (i.e., not indirectly via geometry measurements), to ensure reference values are as close to true as possible. The measurements collected in this experiment help to illustrate how important this point is: during the weighing measurements, each stem was cut into manageable sections, on which length and diameter measurements were made, permitting estimation of geometry-derived (Smalian's formula) green stem mass via the mass-weighted estimate of whole-tree green woody tissue density. We found a percentage error of $-1\,\%$, $7\,\%$, $11\,\%$ and $11\,\%$ when these estimates were compared with direct weighing measurements for T1-T4 respectively. Such large errors in the reference values are dangerous because they could potentially lead to spurious interpretations of the error in lidar- or allometric-derived AGB_{est}.

4.2 Variation in large tropical tree structure

We finish with a brief comment on the interesting insights beyond whole-tree mass, that are provided by the destructive and non-destructive data. For example, we found that for three out of four trees, the bulk of dry mass was most often stored in the crown, with the crown mass ratio ranging from 0.42–0.62 . This absolute variation is consistent with previously published data for large tropical trees in forests similar to our site (e.g., [12]). But the lidar point clouds (figure 2), which provide a unique perspective on tree structure, can begin to offer an insight into this variability. That is, these clouds permit accurate characterisation of crown form: the crown-to-tree height ratio was 0.55, 0.40, 0.54 and 0.56 for T1-T4, and the crown aspect ratio (diameter

of the major axis over crown height) was 1.15, 1.63, 1.18 and 1.44 respectively. A relatively shallower, albeit wider crown then, appears to play some role in explaining why T2 was the only sampled tree with the majority of dry mass found in the stem (it is perhaps also worth noting T2 was the only tree whose crown was found in the emergent layer of the stand). The form of a tree's crown is a result of balancing multiple genetic and ecosystem factors [50], so the highly-accurate QSMs that can be constructed from lidar point clouds (figure 5), which explicitly describe 3D tree architecture through to high order branching, can provide an important platform for ecologists to explore the interaction between tree architecture and controls on ecological function [51, 52].

4.3 Conclusions

In conclusion, we harvested four large tropical rainforest trees in East Amazonia, and weighed whole-tree green mass. We also collected detailed measurements throughout each tree of moisture content and woody tissue density. We found considerable variability in the structure of these trees, including on how AGB was distributed between the stem and crown, and also on the intra- and inter-tree variations in woody tissue density. We acquired 3D laser measurements of each tree prior to harvest, and from these data, estimated tree-scale AGB. We presented the first validation of such estimates from tropical forests using reference values that were derived entirely from direct measurement, and found these estimates provided a 15 −fold improvement in accuracy over counterparts from pan-tropical allometry. We also found error in lidar-derived estimates was not positively correlated with tree size, and reduced when up-scaling to the cumulative AGB of the four trees. If this performance were exhibited at the stand-scale, these new terrestrial lidar methods would enable significantly more accurate estimates of larger-scale carbon stocks. Finally, we suggested that it will be necessary to collect further validation data to generate statistically meaningful out-of-sample uncertainty intervals for lidar-derived AGB predictions.

Data availability

Data from the destructive measurements are archived at https://doi.org/10.5281/zenodo.4056899. Data from the lidar measurements are archived at https://doi.org/10.5281/zenodo.4056903.

Software availability

treeseg is available at https://github.com/apburt/treeseg, and the version used in this paper, v0.2.0, is archived at https://doi.org/10.5281/zenodo.3739213. *TLSeparation* is available at https://github.com/TLSeparation, and the version used in this paper, v1.2.1.5, is archived at https://doi.org/10.5281/zenodo.1147706. *TreeQSM* is available at https://github.com/InverseTampere/TreeQSM, and the version used in this paper, v2.3.2, is archived at https://doi.org/10.5281/zenodo.3560555. *optqsm* is available at https://github.com/apburt/optqsm, and the version used in this paper, v0.1.0, is archived at https://doi.org/10.5281/zenodo.3911269.

Acknowledgements

We thank ICMBio (Instituto Chico Mendes de Biodiversidade) for providing the land to conduct this experiment. We thank the Museu Paraense Emílio Goeldi for providing logistical support. We gratefully acknowledge Cleidemar Araujo de Souza, Filomeno Martins do Amaral Filho, Josenildo Costa Amaral, Juscelino Costa Amaral, Moises Moraes Alves and Raimundo de Souza Brasão Júnior for collecting the harvest data.

Funding

AB and MD acknowledge funding from Natural Environment Research Council (NERC) grant NE/N00373X/1 and European Research Council grant 757526. ACLdC acknowledges funding from Conselho Nacional de Desenvolvimento Científico e Tecnológico (CNPq) grant 457914/2013-0/MCTI/CNPq/FNDCT/LBA/ESECAFLOR. PM acknowledges funding from NERC grant NE/N006852/1. LR acknowledges funding from NERC independent fellowship grant NE/N014022/1. MD also acknowledges funding from NERC National Centre for Earth Observation (NCEO, NE/R016518/1).

Author contributions

All authors designed the methods, and collected and analysed the data. AB wrote the manuscript, with contributions from all authors.

References

1. Saatchi, S. S. *et al.* Benchmark map of forest carbon stocks in tropical regions across three continents. *Proceedings of the National Academy of Sciences* **108,** 9899–9904 (2011).
2. Baccini, A. *et al.* Estimated carbon dioxide emissions from tropical deforestation improved by carbon-density maps. *Nature Climate Change* **2,** 182–185 (2012).
3. Mitchard, E. T. A. *et al.* Markedly divergent estimates of Amazon forest carbon density from ground plots and satellites. *Global Ecology and Biogeography* **23,** 935–946 (2014).
4. Hubau, W. *et al.* Asynchronous carbon sink saturation in African and Amazonian tropical forests. *Nature* **579,** 80–87 (2020).
5. Malhi, Y. *et al.* The regional variation of aboveground live biomass in old-growth Amazonian forests. *Global Change Biology* **12,** 1107–1138 (2006).
6. Avitabile, V. *et al.* An integrated pan-tropical biomass map using multiple reference datasets. *Global Change Biology* **22,** 1406–1420 (2016).
7. Martin, A. R., Doraisami, M. & Thomas, S. C. Global patterns in wood carbon concentration across the world's trees and forests. *Nature Geoscience* **11,** 915–920 (2018).
8. Clark, D. B. & Kellner, J. R. Tropical forest biomass estimation and the fallacy of misplaced concreteness. *Journal of Vegetation Science* **23,** 1191–1196 (2012).
9. Nogueira, E. M., Fearnside, P. M., Nelson, B. W., Barbosa, R. I. & Keizer, E. W. H. Estimates of forest biomass in the Brazilian Amazon: New allometric equations and adjustments to biomass from wood-volume inventories. *Forest Ecology and Management* **256,** 1853–1867 (2008).
10. Saldarriaga, J. G., West, D. C., Tharp, M. L. & Uhl, C. Long-Term Chronosequence of Forest Succession in the Upper Rio Negro of Colombia and Venezuela. *Journal of Ecology* **76,** 938–958 (1988).
11. Brown, I. F. *et al.* Uncertainty in the biomass of Amazonian forests: An example from Rondônia, Brazil. *Forest Ecology and Management* **75,** 175–189 (1995).
12. Maia Araújo, T., Higuchi, N. & Andrade de Carvalho Júnior, J. Comparison of formulae for biomass content determination in a tropical rain forest site in the state of Pará, Brazil. *Forest Ecology and Management* **117,** 43–52 (1999).
13. Chambers, J. Q., dos Santos, J., Ribeiro, R. J. & Higuchi, N. Tree damage, allometric relationships, and above-ground net primary production in central Amazon forest. *Forest Ecology and Management* **152,** 73–84 (2001).
14. Goodman, R. C., Phillips, O. L. & Baker, T. R. The importance of crown dimensions to improve tropical tree biomass estimates. *Ecological Applications* **24,** 680–698 (2014).

15. Brown, S. *Estimating biomass and biomass change of tropical forests. A primer* ISBN: 9789251039557 (FAO - Food and Agriculture Organization of the United Nations, Rome, Italy, 1997).

16. Chave, J. *et al.* Improved allometric models to estimate the aboveground biomass of tropical trees. *Global Change Biology* **20,** 3177–3190 (2014).

17. Slik, J. W. F. *et al.* An estimate of the number of tropical tree species. *Proceedings of the National Academy of Sciences* **112,** 7472–7477 (2015).

18. Feldpausch, T. R. *et al.* Tree height integrated into pantropical forest biomass estimates. *Biogeosciences* **8,** 3381–3403 (2012).

19. Baker, T. R. *et al.* Variation in wood density determines spatial patterns in Amazonian forest biomass. *Global Change Biology* **10,** 545–562 (2004).

20. Phillips, O. L. *et al.* Species Matter: Wood Density Influences Tropical Forest Biomass at Multiple Scales. *Surveys in Geophysics* **40,** 913–935 (2019).

21. Molto, Q., Rossi, V. & Blanc, L. Error propagation in biomass estimation in tropical forests. *Methods in Ecology and Evolution* **4,** 175–183 (2013).

22. Kerkhoff, A. J. & Enquist, B. J. Multiplicative by nature: Why logarithmic transformation is necessary in allometry. *Journal of Theoretical Biology* **257,** 519–521 (2009).

23. Picard, N., Boyemba Bosela, F. & Rossi, V. Reducing the error in biomass estimates strongly depends on model selection. *Annals of Forest Science* **72,** 811–823 (2015).

24. Burt, A. *et al.* Assessment of Bias in Pan-Tropical Biomass Predictions. *Frontiers in Forests and Global Change* **3** (2020).

25. Danson, F. M., Disney, M. I., Gaulton, R., Schaaf, C. & Strahler, A. The terrestrial laser scanning revolution in forest ecology. *Interface Focus* **8** (2018).

26. Wilkes, P. *et al.* Data acquisition considerations for Terrestrial Laser Scanning of forest plots. *Remote Sensing of Environment* **196,** 140–153 (2017).

27. Burt, A., Disney, M. & Calders, K. Extracting individual trees from lidar point clouds using *treeseg. Methods in Ecology and Evolution* **10,** 438–445 (2019).

28. Boni Vicari, M. *et al.* Leaf and wood classification framework for terrestrial LiDAR point clouds. *Methods in Ecology and Evolution* **10,** 680–694 (2019).

29. Krishna Moorthy, S. M., Calders, K., Boni Vicari, M. & Verbeeck, H. Improved Supervised Learning-Based Approach for Leaf and Wood Classification From LiDAR Point Clouds of Forests. *IEEE Transactions on Geoscience and Remote Sensing* **58,** 3057–3070 (2020).

30. Raumonen, P. *et al.* Fast Automatic Precision Tree Models from Terrestrial Laser Scanner Data. *Remote Sensing* **5,** 491–520 (2013).

31. Hackenberg, J., Spiecker, H., Calders, K., Disney, M. & Raumonen, P. SimpleTree - An Efficient Open Source Tool to Build Tree Models from TLS Clouds. *Forests* **6,** 4245–4294 (2015).

32. Plourde, B. T., Boukili, V. K. & Chazdon, R. L. Radial changes in wood specific gravity of tropical trees: inter- and intraspecific variation during secondary succession. *Functional Ecology* **29,** 111–120 (2015).

33. Sagang, L. B. T. *et al.* Using volume-weighted average wood specific gravity of trees reduces bias in aboveground biomass predictions from forest volume data. *Forest Ecology and Management* **424,** 519–528 (2018).

34. Lehnebach, R. *et al.* Wood Density Variations of Legume Trees in French Guiana along the Shade Tolerance Continuum: Heartwood Effects on Radial Patterns and Gradients. *Forests* **10** (2019).

35. Momo Takoudjou, S. *et al.* Leveraging Signatures of Plant Functional Strategies in Wood Density Profiles of African Trees to Correct Mass Estimations From Terrestrial Laser Data. *Scientific Reports* **10** (2020).

36. Calders, K. *et al.* Nondestructive estimates of above-ground biomass using terrestrial laser scanning. *Methods in Ecology and Evolution* **6,** 198–208 (2015).

37. Momo Takoudjou, S. *et al.* Using terrestrial laser scanning data to estimate large tropical trees biomass and calibrate allometric models: A comparison with traditional destructive approach. *Methods in Ecology and Evolution* **9,** 905–916 (2018).

38. Gonzalez de Tanago, J. *et al.* Estimation of above-ground biomass of large tropical trees with terrestrial LiDAR. *Methods in Ecology and Evolution* **9,** 223–234 (2018).

39. Rowland, L. *et al.* Death from drought in tropical forests is triggered by hydraulics not carbon starvation. *Nature* **528,** 119–122 (2015).

40. Meir, P. *et al.* Short-term effects of drought on tropical forest do not fully predict impacts of repeated or long-term drought: gas exchange versus growth. *Philosophical Transactions of the Royal Society B: Biological Sciences* **373** (2018).

41. Chave, J. *et al.* Towards a worldwide wood economics spectrum. *Ecology Letters* **12,** 351–366 (2009).

42. RIEGL Laser Measurement Systems GmbH. *RiSCAN Pro* version 2.7.0. 2018. `http://www.riegl.com`.

43. *CloudCompare* version 2.10.3. 2019. `https://cloudcompare.org/`.

44. Menditto, A., Patriarca, M. & Magnusson, B. Understanding the meaning of accuracy, trueness and precision. *Accreditation and Quality Assurance* **12,** 45–47 (2007).

45. Vieilledent, G. *et al.* New formula and conversion factor to compute basic wood density of tree species using a global wood technology database. *American Journal of Botany* **105,** 1653–1661 (2018).

46. Ter Steege, H. *et al.* Hyperdominance in the Amazonian Tree Flora. *Science* **342** (2013).

47. Schimleck, L. *et al.* Non-Destructive Evaluation Techniques and What They Tell Us about Wood Property Variation. *Forests* **10** (2019).

48. Tuskan, G. A. *et al.* Hardwood Tree Genomics: Unlocking Woody Plant Biology. *Frontiers in Plant Science* **9** (2018).

49. Baison, J. *et al.* Genome-wide association study identified novel candidate loci affecting wood formation in Norway spruce. *The Plant Journal* **100,** 83–100 (2019).

50. Verbeeck, H. *et al.* Time for a Plant Structural Economics Spectrum. *Frontiers in Forests and Global Change* **2** (2019).

51. Meir, P. *et al.* in *Plant Respiration: Metabolic Fluxes and Carbon Balance* (eds Tcherkez, G. & Ghashghaie, J.) 89–105 (Springer International Publishing, 2017). ISBN: 978-3-319-68703-2.

52. Disney, M. Terrestrial LiDAR: a three-dimensional revolution in how we look at trees. *New Phytologist* **222,** 1736–1741 (2019).